Synthesis, Crystal Structures and Magnetic Properties of Composites Incorporating an Fe(II) Spin Crossover Complex and Polyoxometalates

著者	Kuramochi Satoshi, Shiga Takuya, Cameron Jamie, Newton Graham, Oshio Hiroki
journal or publication title	Inorganics
volume	5
number	3
page range	48
year	2017-09
権利	(C)2017 by the authors. Licensee MDPI, Basel, Switzerland. This article is an open access article distributed under the terms and conditions of the Creative Commons Attribution (CC BY) license (http://creativecommons.org/licenses/by/4.0/).
URL	http://hdl.handle.net/2241/00148593

doi: 10.3390/inorganics5030048

inorganics

MDPI

Article

Synthesis, Crystal Structures and Magnetic Properties of Composites Incorporating an Fe(II) Spin Crossover Complex and Polyoxometalates

Satoshi Kuramochi [1], Takuya Shiga [1], Jamie M. Cameron [1], Graham N. Newton [2] and Hiroki Oshio [1,*]

[1] Graduate School of Pure and Applied Sciences, University of Tsukuba, Tennodai 1-1-1, Tsukuba 305-8571, Japan; kurmochi@dmb.chem.tsukuba.ac.jp (S.K.); shiga@chem.tsukuba.ac.jp (T.S.); jamie.c@chem.tsukuba.ac.jp (J.M.C.)

[2] School of Chemistry, University of Nottingham, University Park, Nottingham NG7 2RD, UK; graham.newton@nottingham.ac.uk

* Correspondence: oshio@chem.tsukuba.ac.jp; Tel.: +81-29-853-4238

Received: 30 June 2017; Accepted: 19 July 2017; Published: 22 July 2017

Abstract: $[Fe(dppOH)_2]^{2+}$ (dppOH = 2,6-di(pyrazol-1-yl)-4-(hydroxymethyl)pyridine) is known to show spin crossover (SCO) behavior and light-induced excited spin state transitions (LIESST). Here, we show that the SCO properties of the $[Fe(dppOH)_2]^{2+}$ complex can be altered by a crystal engineering approach employing counter anion exchange with polyoxometalate (POM) anions. Using this strategy, two new composite materials (TBA)$[Fe(dppOH)_2][PMo_{12}O_{40}]$ (**1**) and $[Fe(dppOH)_2]_3[PMo_{12}O_{40}]_2$ (**2**) (TBA = tetra-*n*-butylammonium) have been isolated and studied by single crystal X-ray diffraction and magnetic susceptibility measurements. **1** was found to be in a high spin state at 300 K and showed no spin crossover behavior due to a dense packing structure induced by hydrogen bonding between the hydroxyl group of the dppOH ligands and the POM anions. Conversely, **2** contains two crystallographically unique Fe centers, where one is in the low spin state whilst the other is locked in a high spin state in a manner analogous to **1**. As a result, **2** was found to show partial spin crossover behavior around 230 K with a decrease in the $\chi_m T$ value of 1.9 emu·mol^{-1}·K. This simple approach could therefore provide a useful method to aid in the design of next generation spin crossover materials.

Keywords: spin crossover; polyoxometalate; crystal engineering; magnetic properties; iron

1. Introduction

Spin crossover (SCO) materials have been studied extensively due to their ability to reversibly switch spin states in response to external stimuli, allowing their potential application in molecular electronic devices [1,2]. Spin crossover behavior is often shown in hexacoordinated Fe(II) [3], Fe(III) [4] and Co(II) [5] complexes. Among them, Fe(II) complexes which have dpp ligands (dpp = 2,6-di(pyrazol-1-yl)pyridine) have been widely studied by Halcrow, Howard and co-workers [6–13]. In addition, $[Fe(dpp)_2]^{2+}$ complexes show light-induced excited spin state transitions (LIESST) [8,10], where the spin state can be controllably switched in response to visible light. Significantly, the spin state of the Fe(II) ion is directly affected by the coordination environment and distortions in the plane of the dpp ligand [11,12].

Polyoxometalates (POMs) are large anions in which transition metal cations in their highest oxidation state are bridged by oxo-anions, leading to a huge variety of unique, nano-sized structures [14–16]. POMs are also of interest due to their appealing properties, including reversible, multi-electron redox behavior, electrocatalytic activity [17], photo-oxidizing properties [18,19] and

proton conductivity [20,21], and show great promise for advanced applications. POMs can also act as efficient spacers to magnetically isolate paramagnetic species: for example, Miyasaka, Hayashi and co-workers have recently used POMs as magnetic spacers in Mn^{3+} dimers of a single molecule magnet (SMM) [22].

In this work, the Fe(II) spin crossover complex, $[Fe(dppOH)_2]^{2+}$ (dppOH = 2,6-di(pyrazol-1-yl)-4-(hydroxymethyl)pyridine; Figure 1) and a Keggin-type POM, $[PMo_{12}O_{40}]^{3-}$, are combined to make hybrid composite materials. Specifically, the tridentate ligand dppOH has a pendant hydroxyl group which was expected to show favorable H-bonding interactions with neighboring polyoxoanions. Controlled spin state conversion and modification of the electronic state of $[Fe(dppOH)_2]^{2+}$ were targeted by employing POM anions as crystallographic spacers with potential to display proton acceptor and photo-oxidative properties. Two hybrid materials (TBA)$[Fe(dppOH)_2][PMo_{12}O_{40}]$ (**1**) and $[Fe(dppOH)_2]_3[PMo_{12}O_{40}]_2$ (**2**) (TBA = tetra-*n*-butylammonium), were successfully isolated using a simple synthetic approach. The spin state of the Fe(II) ions in **1** are shown to be high spin across the entire temperature range measured, which is likely due to its highly distorted coordination geometry. Conversely, **2** has three Fe(II) centers, one of which is shown to be stabilized in a low spin configuration and displays moderate partial spin crossover behavior between 100 and 300 K.

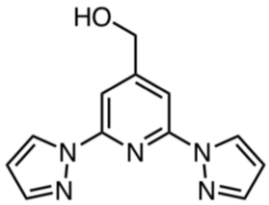

Figure 1. The dppOH (2,6-di(pyrazol-1-yl)-4-(hydroxymethyl)pyridine) ligand.

2. Results

2.1. Synthesis

The tridentate dppOH ligand (dppOH = 2,6-di(pyrazol-1-yl)-4-(hydroxymethyl)pyridine) and the Fe(II) complex, $[Fe(dppOH)_2](BF_4)_2$ were prepared according to previously reported methods [13]. (TBA)$[Fe(dppOH)_2][PMo_{12}O_{40}]\cdot 2CH_3NO_2$ (**1**) and $[Fe(dppOH)_2]_3[PMo_{12}O_{40}]_2\cdot 15H_2O$ (**2**) were synthesized by slow diffusion of the Fe(II) complex into $(TBA)_3[PMo_{12}O_{40}]$ and $H_3PMo_{12}O_{40}$ solutions, respectively. A solution of the POM in 1 mL nitromethane (10 mM) was placed in a glass tube (ϕ = 8 mm), after which a buffer layer of nitromethane and acetonitrile (1:1 *v/v*, 0.5 mL) was layered on top. Finally, a solution of $[Fe(dppOH)_2](BF_4)_2$ in 1 mL acetone/acetonitrile (2:1 *v/v*, 10 mM) was carefully layered on top of the middle buffer layer. After around 1 week, crystals suitable for X-ray analysis were obtained.

2.2. Crystal Structures

The structures of $\mathbf{1}\cdot 2CH_3NO_2$ and $\mathbf{2}\cdot 2CH_3NO_2$ were obtained by single crystal X-ray diffraction at 100 K (Figures 2 and 3). The crystal system of **1** is monoclinic and the space group is $P2_1/c$. The asymmetric unit contains one $[Fe(dppOH)_2]^{2+}$ cation, a TBA cation, a $[PMo_{12}O_{40}]^{3-}$ anion, and two nitromethane solvent molecules. Considering charge balance and BVS (bond valence sum) calculations, the valence of the molybdenum ions can be estimated as 6+, in which the overall charge on the $[PMo_{12}O_{40}]$ anion should be 3−.

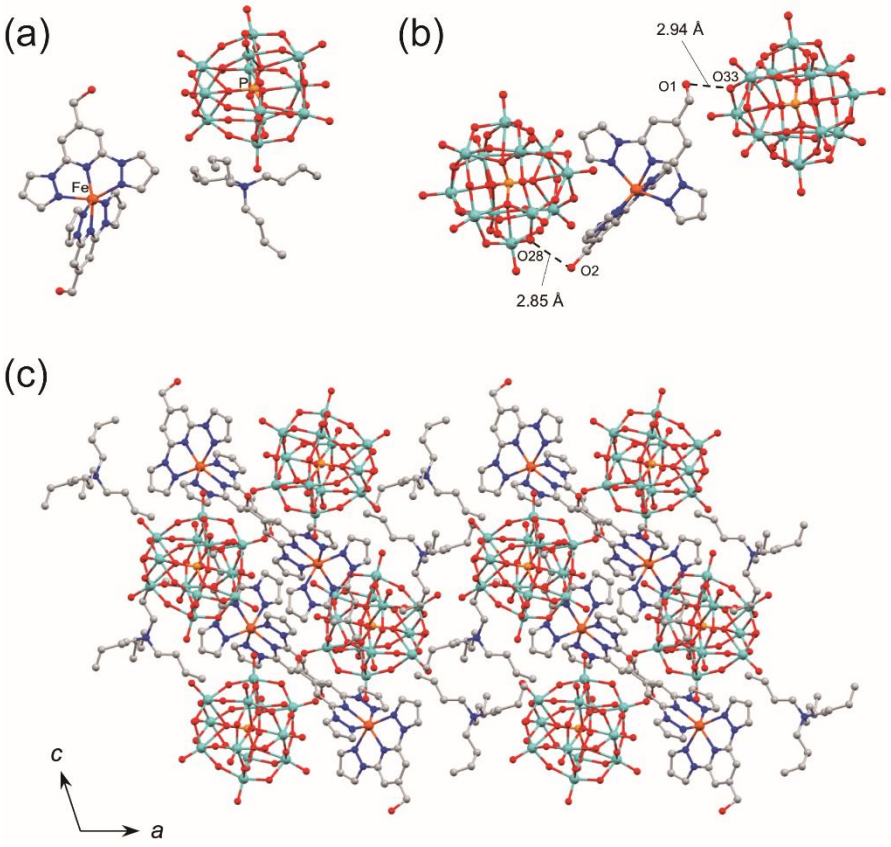

Figure 2. (**a**) X-ray structure of complex **1**; (**b**) hydrogen bonding interactions between $[Fe(dppOH)_2]^{2+}$ and $[PMo_{12}O_{40}]^{3-}$ and (**c**) packing structure of **1** viewed along the crystallographic *b*-axis. Color code: C: gray, N: blue, O: red, P: orange, Fe: brown, Mo: light blue (hydrogen atoms and solvent molecules omitted for clarity).

The Fe(II) ions in **1** were found to be in a distorted octahedral coordination geometry where the angle of *trans*-N(pyridine)–Fe–N(pyridine) (ϕ) and the sum difference of the twelve possible *cis*-N–Fe–N angles (α) from the perpendicular (Σ, where $\Sigma = \Sigma|90 - \alpha|$) [11,12] were found to be $\phi = 158.1°$ and $\Sigma = 151°$, respectively, with an average Fe–N bond length of 2.2 Å. These values are highly typical of high spin Fe(II) and **1** can therefore be assigned as assuming a high spin configuration. In the packing structure of **1**, both pendant hydroxyl groups on the dppOH ligands hydrogen bond to a bridging μ_2-oxo group on the $[PMo_{12}O_{40}]^{3-}$ anion (Figure 2b), where the distance between the oxygen atoms of the hydroxyl groups and the μ_2-oxo bridges ($d_{O1 \ldots O33}$ and $d_{O2 \ldots O28}$) are 2.94 Å and 2.85 Å, respectively. The dense packing arrangement observed in **1** leads to distorted coordination structure, exerting a strong influence on the coordination environment parameters of the Fe(II) centers and stabilizes its high-spin state.

The crystal system of $\mathbf{2}{\cdot}2CH_3NO_2$, which was synthesized with the free acid of the POM ($[H_3PMo_{12}O_{40}]$) as a starting material, is monoclinic with space group $C2/c$. The asymmetric unit contains one and a half $[Fe(dppOH)_2]^{2+}$ cationic units and one full $[PMo_{12}O_{40}]^{3-}$ anionic unit, in addition to one nitromethane molecule. **2** also contains two crystallographically distinct Fe(II) centers, Fe1 and Fe2. As discussed above, the coordination geometry parameters ϕ and Σ were found to be $\phi = 176.1°$ and $\Sigma = 87°$ for Fe1, while those of Fe2 were found to be $\phi = 156.4°$ and $\Sigma = 158°$. The average Fe1–N and Fe2–N bond lengths are 1.9 Å and 2.2 Å, respectively, at 100 K. In this case, the observed values for Fe1 and Fe2 suggest the existence of both low-spin and high-spin states in the Fe(II) ions, respectively. It can also be noted that Fe1 is located on the center of symmetry and shows

no H-bonding interactions between [Fe(dppOH)$_2$] and the POM cluster, while Fe2 shows hydrogen bonding interactions at the pendant hydroxyl groups, analogous to those in compound **1**.

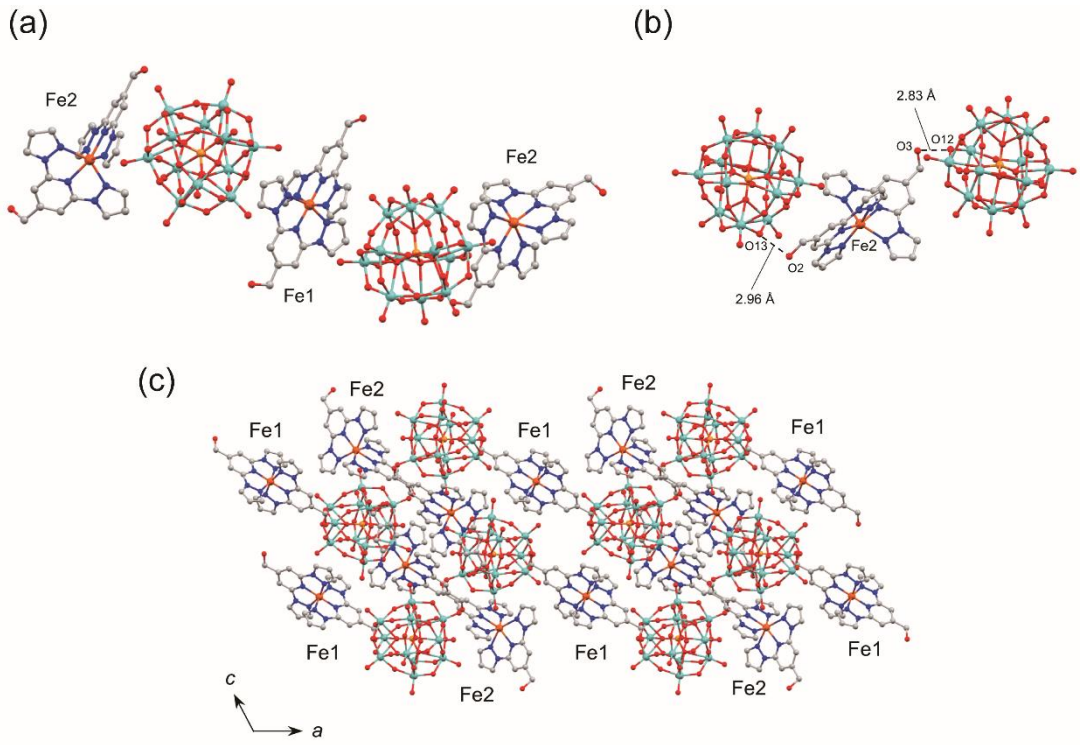

Figure 3. (**a**) X-ray structure of **2**; (**b**) hydrogen bonding interactions between Fe2-complexes and $[PMo_{12}O_{40}]^{3-}$ and (**c**) the packing structure of **2** viewed along the crystallographic *b*-axis. Color code: C: gray, N: blue, O: red, P: orange, Fe: brown, Mo: light blue (hydrogen atoms and solvent molecules omitted for clarity).

2.3. Temperature Dependence of the Magnetic Susceptibilities

The temperature dependence of the magnetic susceptibility was measured for both **1** and **2** in the range of 1.8–300 K (Figure 4). At 300 K, the $\chi_m T$ value of **1** is 4.51 emu·mol^{-1}·K (g = 2.45). This value confirms that the Fe(II) ion of **1** is in a high spin state (S = 2). At temperatures above 30 K, the $\chi_m T$ value is constant, while below 30 K it decreases sharply due to intermolecular interactions and/or zero-field splitting effects associated with the Fe(II) ions. The $\chi_m T$ value of **2** at 300 K was found to be slightly low for three isolated high spin Fe(II) ions at 11.05 emu·mol^{-1}·K, suggesting that **2** may not be in a fully high spin state at 300 K (i.e., the spin state of **2** may be more accurately described as $(2 + x)$ HS Fe^{II} + $(1 - x)$ LS Fe^{II}). Furthermore, upon cooling, the $\chi_m T$ value of **2** gradually decreases to 9.11 emu·mol^{-1}·K at 100 K, and this magnetic behavior can be ascribed to partial thermal spin crossover behavior. From this data, it can be suggested that **2** contains one low-spin Fe(II) ion and two high-spin Fe(II) ions (g = 2.46) at 100 K, whilst at higher temperatures (300 K), a fraction of low spin Fe(II) ions may undergo thermally-driven spin crossover to the high spin state.

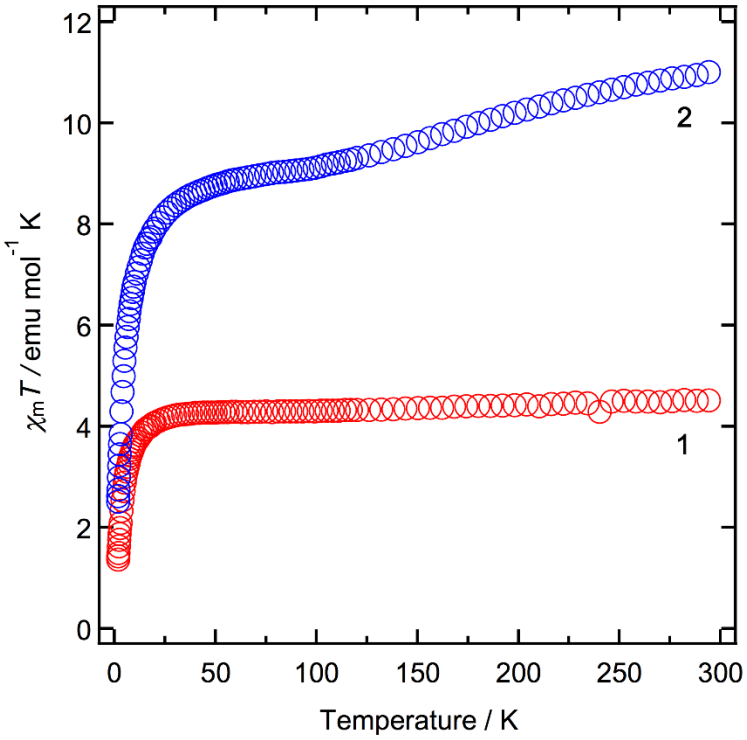

Figure 4. Temperature dependence of the $\chi_m T$ product for **1** (red) and **2** (blue).

3. Discussion

It was previously reported that the analogous complexes $[Fe(dppOH)_2](BF_4)_2$ and $[Fe(dppOH)_2](HClO_4)_2$ show spin crossover behavior with $T_{1/2}$ = 271 K and 284 K, respectively [10], whilst the Fe(II) ion in **1** is "locked" in the high-spin state and shows no spin crossover behavior. It follows that the high spin state of Fe(II) is therefore stabilized in the crystal structure of **1,** and we have considered the following explanations. Firstly, the influence of the packing structure formed by the $[Fe(dppOH)_2]^{2+}$ cations and $[PMo_{12}O_{40}]^{3-}$ anions is crucial. From our results, it appears clear that close-packing and H-bonding interactions between the POM clusters and the hydroxyl groups on the pendant (dppOH) ligands lead to significant distortion in the coordination environment of the Fe(II) ions (ϕ = 158.1°, Σ = 151°). This highly-distorted coordination geometry around the Fe(II) ion stabilizes a high-spin state at all temperatures. In the case of compound **1**, the uniform 1:1 dense packing arrangement of the $[Fe(dppOH)_2]$ and POM units (seen clearly in Figure 2b) facilitated by these close-packing interactions is supported by an additional layer of charge-balancing TBA cations which can be found in a distinct intermediate space between the groups of closely-associated POM and $[Fe(dppOH)_2]^{2+}$ moieties.

On the other hand, **2** is shown to exhibit partial spin crossover behavior. In the crystal structure of **2** at 100 K, two high-spin Fe(II) moieties (Fe2) and one low-spin Fe(II) center (Fe1) can be identified. Where the crystal structure of **2** is similar to that of **1** (in which an observably similar 1:1 dense packing arrangement can be found between the Fe2-complexes and the POM anions), a highly distorted coordination geometry around the Fe2 ions is favored which stabilizes a high spin state in a manner analogous to that in compound **1** (ϕ = 156.4° and Σ = 158°). Conversely, the Fe1 complexes show no significant intermolecular interactions with the POM counter-anions (with a minimum distance d_{O-O} = 3.52 Å between the POM and the pendant hydroxyl group on the dppOH ligands) and are located in a larger crystallographic space (analogous to the TBA cations in compound **1**), with markedly less dense packing than the Fe2 complexes (see Figure 3). As a result, the Fe1 ions experience minimal distortion (ϕ = 176.1° and Σ = 87°) and the structural changes associated with the spin crossover of the

Fe2 complex are unhindered. As a result, the Fe2 complexes show moderate spin crossover behavior with an estimated $T_{1/2}$ value ≈ 230 K. We attempted to explore the details of these structural changes by single crystal structural analysis, however it failed as the result of **2** having lost crystallinity at 300 K. In addition, Mössbauer spectroscopy could not be employed in this instance to aid elucidation of the electronic state of the Fe ions because the Mo-containing POM clusters strongly absorb γ-rays.

4. Materials and Methods

4.1. Materials

The dppOH ligand and Fe(II) SCO complex, $[Fe(dppOH)_2](BF_4)_2$ were synthesized according to the literature methods [13]. $(TBA)_3[PMo_{12}O_{40}]$ was synthesized by performing a simple cation exchange by adding excess TBABr to an aqueous solution of $H_3PMo_{12}O_{40}{\cdot}nH_2O$ and collecting the resulting yellow precipitate by vacuum filtration. All other chemicals and solvents are commercially available and were used as received without further purification.

4.2. Synthesis of [Fe(dppOH)$_2$][POM] Composites

$(TBA)[Fe(dppOH)_2][PMo_{12}O_{40}]{\cdot}2CH_3NO_2$ (**1**): A solution of $(TBA)_3[PMo_{12}O_{40}]$ (255 mg, 0.10 mmol) in 10 mL nitromethane was prepared and then separated into 10 equal batches in glass tubes (ϕ = 8 mm). A mixture of nitromethane and acetonitrile (1:1 *v/v*, 0.5 mL) was then layered on top of the POM solution as a buffer layer to facilitate slow diffusion. Finally, a pre-prepared solution of $[Fe(dppOH)_2](BF_4)_2$ (95 mg, 0.13 mmol) in 10 mL acetone/acetonitrile (2:1 *v/v*) was separated into 10 equal batches and carefully layered on top of the buffer layer. The vials were then sealed and left undisturbed, and after approximately one week, yellow crystals of **1** suitable for X-ray analysis were obtained. The crystalline sample was collected via pipette and dried under vacuum prior to analysis (yield = 55 mg, 15%). Anal. Calcd. for $\mathbf{1}{\cdot}2CH_3NO_2$, $C_{42}H_{64}N_{13}FeMo_{12}O_{46}P$; C, 18.51; H, 2.37; N, 6.68. Found: C, 19.34; H, 2.11; N, 6.32.

$[Fe(dppOH)_2]_3[PMo_{12}O_{40}]_2{\cdot}15H_2O$ (**2**): A solution of $H_3PMo_{12}O_{40}{\cdot}nH_2O$ (190 mg) in 10 mL nitromethane was separated into 10 equal batches and placed in glass tubes (ϕ = 8 mm). A mixture of nitromethane and acetonitrile (1:1 *v/v*, 0.5 mL) was layered on top of the POM solution as a buffer layer to facilitate slow diffusion. Finally, a solution of $[Fe(dppOH)_2](BF_4)_2$ (95 mg, 0.13 mmol) in 10 mL acetone/acetonitrile (2:1 *v/v*) was separated into 10 equal batches and carefully layered on top of the buffer layer. After approximately 1 week, yellow crystals of **2** suitable for X-ray analysis were obtained. The crystalline sample was collected via pipette and dried under vacuum prior to analysis (yield = 33 mg, 4%). Anal. Calcd. for $\mathbf{2}{\cdot}15H_2O$, $C_{72}H_{96}N_{30}Fe_3Mo_{24}O_{101}P_2$; C, 15.64; H, 1.75; N, 7.60. Found: C, 15.77; H, 1.36; N, 7.15. We note that the elemental analysis was measured after the samples had been dried under vacuum and that, whilst care was taken in all cases to measure the dry material as promptly as possible, re-exposure to ambient conditions might help to explain the anomalous hydration of the sample (as is best fitted to the elemental analysis data) when compared to the single crystal data, where two nitromethane molecules are found per formula unit.

4.3. X-ray Crystallography

Crystals were mounted in oil on a micromount, and data were collected at 100 K on a SMART APEXII diffractometer (Bruker, Billerica, MA, USA) coupled with a CCD area detector and with graphite monochromated Mo Kα (λ = 0.71073 Å) radiation. The structure was solved using direct methods and expanded using Fourier techniques within the *SHELXTL* program [23]. Empirical absorption corrections were calculated using SADABS. In the structure analyses, non-hydrogen atoms were refined with anisotropic thermal parameters. Hydrogen atoms were included in calculated positions and refined with isotropic thermal parameters riding on those of the parent atoms.

Full details of the crystallographic analysis and accompanying cif files may be obtained free of charge from the Cambridge Crystallographic Data Centre (CCDC numbers 1559207 and 1559208) via

http://www.ccdc.cam.ac.uk/conts/retrieving.html (or from the CCDC, 12 Union Road, Cambridge CB2 1EZ, UK; Fax: +44 1223 336033; E-mail: deposit@ccdc.cam.ac.uk).

4.4. Magnetic Measurements

Variable-temperature magnetic susceptibility measurements were carried out on polycrystalline samples under an applied field of 20,000 Oe using an MPMS-XL SQUID magnetometer (Quantum Design, San Diego, CA, USA). Diamagnetic corrections for the sample holder and $[PMo_{12}O_{40}]^{3-}$ were collected experimentally and the contribution of the TBA cations and the (dppOH) ligands were calculated using Pascal's constants. Data collections were conducted at a rate of 1 K/min.

5. Conclusions

New composite crystals **1** and **2**, incorporating spin crossover Fe(II) complexes and POM anions were synthesized and their crystal structures have been obtained at 100 K. While $[Fe(dppOH)_2](BF_4)_2$ shows high-spin to low-spin SCO behavior with $T_{1/2}$ = 271 K, **1** is trapped in the high-spin state below 300 K and shows no spin crossover behavior. **2** contains three $[Fe(dppOH)_2]$ cations per formula unit, two of which are similarly locked in the high-spin state configuration whilst the remaining Fe(II) ion is found to exist in a low-spin state at 100 K and shows partial spin crossover behavior. The coordination geometry around the Fe(II) ions is strongly affected by interactions between the pendant hydroxyl groups of the dppOH ligand and the POM anions, which has a direct result on the spin state of the composite compound. From this result, we show that combining spin crossover complexes with functional anions can be used to modify spin crossover properties, and future work will demonstrate how switchable behaviors can be obtained by facilitating proton-transfer interactions between the ligand and the POM.

Supplementary Materials: The following are available online at www.mdpi.com/2304-6740/5/3/48/s1. Cif and cif-checked files.

Acknowledgments: This work was supported by JSPS KAKENHI Grant Number JP16H06523 (Coordination Asymmetry). This work was also supported by Grant-in-Aid for JSPS Research Fellow Grant Number J02555. (Satoshi Kuramochi) and a JSPS Postdoctoral Fellowship for Foreign Researchers (Jamie M. Cameron).

Author Contributions: Hiroki Oshio conceived and supervised the project. Satoshi Kuramochi and Takuya Shiga conducted and interpreted the synthetic and analytical experiments. Jamie M. Cameron and Graham N. Newton provided assistance in the direction of the project. Satoshi Kuramochi prepared the manuscript with assistance from Takuya Shiga and Jamie M. Cameron.

Conflicts of Interest: The authors declare no conflict of interest.

References

1. Real, J.; Gaspar, A.; Muñoz, C.M. Thermal, Pressure and Light Switchable Spin-Crossover Materials. *Dalton Trans.* **2005**, 2062–2079. [CrossRef] [PubMed]
2. Bousseksou, A.; Molnár, G.; Salmon, L.; Nicolazzi, W. Molecular Spin Crossover Phenomenon: Recent Achievements and Prospects. *Chem. Soc. Rev.* **2011**, *40*, 3313–3335. [CrossRef] [PubMed]
3. Halcrow, M.A. The Spin-States and Spin-Transitions of Mononuclear Iron(II) Complexes of Nitrogen-Donor Ligands. *Polyhedron* **2007**, *26*, 3523–3576. [CrossRef]
4. Nihei, M.; Shiga, T.; Maeda, Y.; Oshio, H. Spin Crossover Iron(III) Complexes. *Coord. Chem. Rev.* **2007**, *251*, 2606–2621. [CrossRef]
5. Krivokapic, I.; Zerara, M.; Daku, M.; Vargas, A.; Enachescu, C.; Ambrus, C.; Tregenna-Piggott, P.; Amstutz, N.; Krausz, E.; Hauser, A. Spin-Crossover in Cobalt(II) Imine Complexes. *Coord. Chem. Rev.* **2007**, *251*, 364–378. [CrossRef]
6. Holland, J.M.; McAllister, J.A.; Lu, Z.; Kilner, C.A.; Thornton-Pett, M.; Halcrow, M.A. An Unusual Abrupt Thermal Spin-State Transition in $[FeL_2][BF_4]_2$ [L = 2,6-Di(Pyrazol-1-yl)Pyridine]. *Chem. Commun.* **2001**, 577–578. [CrossRef]

7. Holland, J.M.; McAllister, J.A.; Kilner, C.A.; Thornton-Pett, M.; Bridgeman, A.J.; Halcrow, M.A. Stereochemical Effects on the Spin-State Transition Shown by Salts of $[FeL_2]^{2+}$ [L = 2,6-Di(Pyrazol-1-yl)Pyridine]. *J. Chem. Soc. Dalton Trans.* **2002**, 548–554. [CrossRef]
8. Money, V.A.; Elhaïk, J.; Halcrow, M.A.; Howard, J.A.K. The Thermal and Light Induced Spin Transition in $[FeL_2](BF_4)_2$ (L = 2,6-Dipyrazol-1-yl-4-Hydroxymethylpyridine). *Dalton Trans.* **2004**, 1516–1518. [CrossRef] [PubMed]
9. Halcrow, M.A. The Synthesis and Coordination Chemistry of 2,6-Bis(Pyrazolyl)Pyridines and Related Ligands—Versatile Terpyridine Analogues. *Coord. Chem. Rev.* **2005**, *249*, 2880–2908. [CrossRef]
10. Carbonera, C.; Costa, J.; Money, V.A.; Elhaïk, J.; Howard, J.A.K.; Halcrow, M.A.; Létard, J.-F. Photomagnetic Properties of Iron(II) Spin Crossover Complexes of 2,6-Dipyrazolylpyridine and 2,6-Dipyrazolylpyrazine Ligands. *Dalton Trans.* **2006**, 3058–3066. [CrossRef] [PubMed]
11. Halcrow, M.A. Structure: Function Relationships in Molecular Spin-Crossover Complexes. *Chem. Soc. Rev.* **2011**, *40*, 4119–4142. [CrossRef] [PubMed]
12. Cook, L.J.; Mohammed, R.; Sherborne, G.; Roberts, T.D.; Alvarez, S.; Halcrow, M.A. Spin State Behavior of Iron(II)/Dipyrazolylpyridine Complexes. New Insights from Crystallographic and Solution Measurements. *Coord. Chem. Rev.* **2015**, *289*, 2–12. [CrossRef]
13. Nihei, M.; Maeshima, T.; Kose, Y.; Oshio, H. Synthesis, Structure and Magnetic Properties of an Iron(II) Complex with Nitronyl Nitroxides. *Polyhedron* **2007**, *26*, 1993–1996. [CrossRef]
14. Pope, M.T.; Müller, A. Polyoxometalate Chemistry: An Old Field with New Dimensions in Several Disciplines. *Angew. Chem. Int. Ed.* **1991**, *30*, 34–48. [CrossRef]
15. Tzirakis, M.D.; Lykakis, I.N.; Orfanopoulos, M. Decatungstate as an Efficient Photocatalyst in Organic Chemistry. *Chem. Soc. Rev.* **2009**, *38*, 2609–2621. [CrossRef] [PubMed]
16. Long, D.L.; Tsunashima, R.; Cronin, L. Polyoxometalates: Building Blocks for Functional Nanoscale Systems. *Angew. Chem. Int. Ed.* **2010**, *49*, 1736–1758. [CrossRef] [PubMed]
17. Sadakane, M.; Steckhan, E. Electrochemical Properties of Polyoxometalates as Electrocatalysts. *Chem. Rev.* **1998**, *98*, 219–238. [CrossRef] [PubMed]
18. Yamase, T. Photoredox Chemistry of Polyoxometalates as a Photocatalyst. *Catal. Surv. Asia* **2003**, *7*, 203–217. [CrossRef]
19. Streb, C. New Trends in Polyoxometalate Photoredox Chemistry: From Photosensitisation to Water Oxidation Catalysis. *Dalton Trans.* **2012**, *41*, 1651–1659. [CrossRef] [PubMed]
20. Nakamura, O.; Kodama, T.; Ogino, I.; Miyake, Y.; Nakamura, O.; Kodama, T.; Ogino, I.; Miyake, Y. High-Conductivity Solid Proton Conductors: Dodecamolybdophosphoric Acid and Dodecatungstophosphoric Acid Crystals. *Chem. Lett.* **1979**. [CrossRef]
21. Miras, H.N.; Yan, J.; Long, D.-L.L.; Cronin, L. Engineering Polyoxometalates with Emergent Properties. *Chem. Soc. Rev.* **2012**, *41*, 7403–7430. [CrossRef] [PubMed]
22. Sawada, Y.; Kosaka, W.; Hayashi, Y.; Miyasaka, H. Coulombic Aggregations of Mn^{III} salen-Type Complexes and Keggin-Type Polyoxometalates: Isolation of Mn_2 Single-Molecule Magnets. *Inorg. Chem.* **2012**, *51*, 4824–4832. [CrossRef] [PubMed]
23. Sheldrick, G. A short history of *SHELX*. *Acta Crystallogr. Sect. A* **2008**, *64*, 112–122. [CrossRef] [PubMed]